Comparison between intensity and pressure as measures of sound level in the ear canal

Stephen T. Neely[a] and Michael P. Gorga
Boys Town National Research Hospital, 555 North 30 Street, Omaha, Nebraska 68131

(Received 12 March 1998; accepted for publication 28 July 1998)

In-the-ear calibration of sound pressure level may be problematic at frequencies above 2 kHz, because the pressure can vary significantly along the length of the ear canal, due to reflection of sound waves at the eardrum. This issue has been investigated by measuring behavioral thresholds to tones in a group of human subjects ($N=61$) for two different insertion depths of an insert earphone. The change in insertion depth was intended to alter the distribution of pressure in the ear canal, shifting the frequency at which spectral notches occur. The inset earphone or ''probe'' (Etymotic ER-10C) also contained a calibrated microphone, allowing the recording of sound pressure levels in the ear canal. Prior to the threshold measurements in each subject, the Thevenin acoustic source characteristics of the probe were determined by a special calibration procedure. This calibration allowed the expression of the sound level at threshold in terms of acoustic intensity (W/m^2). The impact of changes in insertion depth was determined by measuring behavioral threshold at each depth. Because cochlear sensitivity remained constant, the level of sound entering the ear at threshold should have been the same (within measurement error) for both insertions. The difference in sound pressure level (SPL) at threshold between the two probe insertions was greatest at the notch frequency of the first insertion. At this notch frequency, the SPL at threshold increased by an average of 11.4 dB. The change in sound intensity level (SIL) at threshold was almost always less than the change in SPL. At the notch frequency, the SIL decreased, on average, by only 0.5 dB. These results suggest that SIL may be a better indicator than SPL of the sound level entering the ear, especially for frequencies in the 4–8 kHz range. [S0001-4966(98)03011-2]

PACS numbers: 43.64.Ha, 43.64.Jb, 43.64.Yp [BLM]

INTRODUCTION

In-the-ear sound pressure calibration has become increasingly popular in recent years due to the availability of high quality, calibrated probe microphones (e.g., Etymotic ER-7C and ER-10C). It is generally agreed that the pressure at the eardrum is a better measure of the stimulus than the pressure at the earphone (e.g., Siegel, 1994). However, due to the difficulty of measuring sound pressure at the eardrum, the pressure at the earphone is often used to calibrate stimuli. For example, most commercial distortion-product otoacoustic emission (DPOAE) systems rely on pressure at the earphone for stimulus calibration.

The accuracy with which pressure measurements at the earphone estimate the pressure at the eardrum is frequency dependent (Siegel, 1994; Siegel and Hirohata, 1994). For frequencies below about 2 kHz, pressure throughout the ear canal is more nearly uniform, because the quarter wavelength of the signal is large compared with the dimensions of the ear canal. This situation does not exist at higher frequencies, where standing waves can result in a partial cancellation of the sound pressure seen at the microphone. As a result, the pressure seen at the measurement microphone could potentially underestimate the pressure at the eardrum for these higher frequencies. Obviously, the dimensions of the ear canal also influence the accuracy of these measurements. All other things being equal, the upper frequency limit for which pressure measurements at the plane of the probe indicate pressure at the eardrum will decrease as the length of the ear canal increases.

An alternative measure of stimulus level is acoustic *intensity*, defined as the acoustic power per unit area (e.g., W/m^2). Intensity at the earphone will be a good indicator of the intensity at the eardrum whenever ear canal losses are small (Keefe *et al.*, 1993). It is expected that specifying the stimulus level in terms of acoustic power avoids the problem of standing wave notches (e.g., Marlan *et al.*, 1994). However, power measurements require more information about the acoustic load than pressure measurements. Microphones directly measure acoustic *pressure*. To convert a pressure measurement into a power or intensity value, the *conductance* of the acoustic load must also be determined. One way to estimate the conductance of the load is to first calibrate the acoustic source characteristics of the probe (Møller, 1960; Rabinowitz, 1981; Allen, 1986; Keefe *et al.* 1992).

The probe can be characterized by its Thevenin-equivalent source pressure and source impedance (Allen, 1986). These source parameters can be estimated by a special calibration procedure which uses a set of acoustic cavities to provide known acoustic loads (Allen, 1986). Once the source parameters are known, the probe can be used to measure the conductance of any given acoustic load.

The study described in this paper investigates two related questions: (1) How well do sound pressure measure-

[a]Electronic mail: neely@boystown.org.

ments in the ear canal describe the level of sound that enters the ear? and (2) Do sound intensity measurements provide a better (i.e., more reliable) description of stimulus level than sound pressure measurements? To investigate these questions, we used behavioral threshold to maintain a nearly constant level of sound entering the ear and manipulated the distribution of pressure in the ear canal by varying the insertion depth of an insert earphone and microphone (probe). Since it is assumed that behavioral thresholds do not vary (at least within a test session), any variances in behavioral threshold must reflect inaccuracy in the calibration procedure. By calibrating in both SPL and SIL, we can compare the relative accuracy of pressure and intensity measurements over a wide range of frequencies.

I. METHODS

A. Probe

An ER-10C probe microphone (Etymotic Research) was used to deliver stimuli and to measure sound pressure level in the ear canal. This microphone is well suited for making pressure measurements because it has a nearly constant sensitivity of about 0.05 V/Pa, over a wide range of frequencies. This means that at the output of the preamp, a measurement expressed in terms of dB *re*: μV can be interpreted as a measurement of dB SPL (*re*: 20 μPa).

The Thevenin acoustic source characteristics were estimated (using locally developed software) for the ER-10C probe by a method similar to the one described by Allen (1986). [See also Keefe *et al.* (1992) and Voss and Allen (1994).] Five brass tubes (11/32 in. o.d., 8 mm i.d.) of varying lengths (21, 24, 28, 34, and 42 mm) were closed at one end and mounted vertically for use as acoustic cavities by gluing one end of each tube to a single brass plate.

In order to attach the ER-10C probe to the open ends of the calibration tubes, a simple coupler was made by gluing a short (20 mm) section of the same diameter tube inside a slightly longer (30 mm) section of the next larger diameter tube (3/8 in. o.d.). The foam eartip of the ER-10C probe was compressed and inserted into the smaller end of the coupler. The larger end of the coupler was seated on top of the open end of the acoustic cavity providing a good acoustic seal between the probe and the cavity. The coupler effectively extended the tube length by about 3 mm.

The pressure response of each of the five cavities to a wide-band chirp stimulus was measured by the ER-10C microphone. The stimulus was generated and the response recorded digitally by a Turtle Beach ''Tahiti'' soundcard at a sample rate of 44.1 kHz. Although the ER-10C probe contains two receivers (loudspeakers), only one receiver was used in this study. The chirp stimulus delivered to the receiver was 112-mV peak-to-peak (40-mV rms) with a flat spectrum from 0 to 20 kHz. Synchronous averaging of repeated stimuli was used to reduce noise in the calibration measurement. The total averaging time was about 37 s per chirp-response measurement (corresponding to 80 repetitions of a 46.4-ms chirp).

Because the probe calibration is sensitive to temperature, the acoustic cavities were maintained at a temperature between 34 and 40 °C (monitored by an oral thermometer inserted into the tallest tube). This was intended to warm the *probe* to approximately the same temperature during calibration as when it was inserted into a human ear canal. As a result, the speed of sound in the interior air spaces of the probe should have been about the same during probe calibration as when the probe was inserted into an ear canal.

The acoustic impedance of each cavity was computed by a formula derived by Keefe (1984). This formula requires that the length, diameter, and temperature of the tubes be known. The length of the acoustic cavities (including the coupler) could not be determined with sufficient accuracy by direct measurement, so an initial estimate of this length, based on the frequency of the first prominent spectral peak, was subsequently improved by numerical iteration. The procedure used an overspecified set of five linear equations, based on both the measured cavity pressures and the calculated cavity impedances, to generate an error term, and sought to minimize the error by adjusting the estimated tube lengths iteratively (Allen, 1986). The Thevenin source impedance and pressure for the ER-10C probe was determined by this procedure.

Acoustic intensity is, in general, a vector quantity equal to the product of fluid velocity and pressure. In this paper, we consider only the direction normal to the plane of the probe and treat intensity as a scalar quantity. For a particular frequency component, intensity can be computed as

$$I(f)=\tfrac{1}{2}\mathrm{Re}[v(f)^{*}\cdot p(f)],$$

where $v(f)$ and $p(f)$are, respectively, the complex Fourier components of velocity and pressure at that frequency. (Re[] extracts the real part of a complex number, and the * denotes a complex conjugate.) *Specific* acoustic impedance (or unit area acoustic impedance) is defined as the ratio of the pressure and velocity

$$Z_s(f)=\frac{p(f)}{v(f)}$$

(Pierce, 1981). If the specific impedance is known, then intensity can be computed as

$$I(f)=G_s(f)\cdot p_{\mathrm{rms}}^2(f),$$

where $p_{\mathrm{rms}}(f)$is the rms pressure and $G_s(f)=\mathrm{Re}[Z_s^{-1}(f)]$ is the specific conductance. The specific impedance of air (at 37 °C) is $\rho c=401$ Pa s/m (Keefe, 1984).

The characteristic impedance of the brass tubes used for probe calibration is $Z_0=\rho c/A_0=8.0\times10^6$ Pa s/m^3 (=80 cgs acoustic ohms) where $A_0=5.0\times10^{-5}$ m^2 is the cross-sectional area of each tube. The source impedance of the probe Z_{prb} and the load impedance of the ear canal Z_{ec}, which are derived from the calibration procedure, have the same units as Z_0. For simplicity, the source and load impedances are normalized by Z_0 when they are presented in Sec. II.

Because the foam eartip was changed for each subject, the probe calibration was repeated for each subject either immediately before or immediately after behavioral threshold measurements were made. The entire probe calibration procedure was completed in about 5–10 min.

B. Subjects

Subjects were seated in a comfortable chair in a sound-attenuating booth. The ER-10C probe (with the same foam eartip that was used for probe calibration) was inserted into the subject's ear canal. Special effort was made to obtain an initial insertion as deep as possible. A pressure response was measured in the ear canal using the same wide-band chrip stimulus. The ear canal (load) pressure, together with the previously determined source pressure and impedance, provided enough information to calculate the specific conductance of the ear canal. The *notch frequency* was identified by a peak in the conductance curve in the 1–8 kHz range. Conductance was used to determine the notch frequency instead of pressure because the conductance maximum was easier to locate. The notch occurs in the pressure magnitude (versus frequency) curve because reflected sound from the eardrum arrives back at the probe with a 180 degrees phase shift at this frequency and tends to cancel the forward-going sound being emitted by the probe. This sound-wave cancellation is also responsible for the observed peak in the conductance curve.

Following the measurements of the ear canal pressure response, behavioral threshold measurements were made. The subjects were asked to press a response button each time they heard a tone. The tones were presented 100 times at each of 12 frequencies. The tone was initially presented at 40 dB SPL, decreased in level on the next trial by 5 dB if the subject indicated that the tone was heard, and increased by 5 dB if the subject did not respond. The 1-s interval between tones was extended if the subject had not yet released the button. Thresholds were measured at the five octave frequencies from 0.5 to 8 kHz and at seven additional frequencies in the vicinity of the notch frequency. The first set of ear canal calibration and threshold measurements required about 35 min to complete.

The seven additional frequencies extended from one octave below to one-half octave above the notch frequency in quarter-octave steps. This asymmetric pattern was selected to maximize our observations around the notch frequencies of both probe insertions, where we expected the calibration errors to be greatest. The second probe insertion was always less deep than the first insertion and was expected to have a notch frequency about one-half octave lower than the notch frequency of the first insertion. By designing our threshold estimates to extend one octave below the initial notch frequency, we expected the estimates to also extend one-half octave below the notch frequency of the second insertion.

Thresholds were determined by a maximum-likelihood procedure (Green, 1993). Likelihood values, based on all 100 trials, were computed using a logistic function to approximate the psychometric function describing percent of ''yes'' votes (Green, 1995). The parameters of the logistic function were (1) upper asymptote, (2) lower asymptote, (3) slope, and (4) threshold. Values for these four parameters were chosen by numerical iteration to obtain a maximum likelihood value, given the history of responses to the 100 trials. The threshold of the psychometric function with the maximum likelihood was selected as the behavioral threshold for that tone.

After a short break, the probe was again inserted into the subjects' ear canal, but this time not as deep as the first time. During this probe insertion procedure, a new notch frequency (determined from the conductance peak) was computed online and updated on the computer screen every few seconds. The insertion depth was adjusted until the notch frequency shifted (usually downward) by about $\frac{1}{2}$ octave (at least $\frac{1}{4}$ and not more than $\frac{3}{4}$ octave), compared to the initial probe insertion. The ear canal conductance and threshold at the same 12 frequencies were again measured in the same way as they were for the initial deeper insertion.

The threshold measurements provided a way to control the level of the sound entering the ear that was independent of any measurements from the probe microphone. We assumed that behavioral threshold over the duration of a test session was relatively constant. Therefore, any difference in threshold between the two probe insertions could not be a consequence of a change in middle-ear or cochlear function. The threshold differences can be attributed to two sources (1) threshold estimation errors and (2) calibration errors. The threshold estimation errors should be unbiased (i.e., equally likely to be larger or smaller for the second insertion). Therefore, any tendency for the pressure or intensity at threshold to be consistently larger or smaller for the second insertion must reflect an error in the corresponding pressure or intensity calibration. The extent to which the behavioral thresholds vary provides an estimate of the error in the pressure (SPL) or intensity (SIL) calibration.

The experimental protocol was completed on 75 subjects ranging in age from 14 to 78 years. All subjects were presumed to have ''normal'' hearing, based on informal questioning; however, this was not confirmed by clinical audiometric assessment because normal hearing was not a requirement for this experiment. It was only necessary for the subjects to be able to hear the tones and for their threshold to remain constant over the course of participation in the experiment, which typically lasted less than 2 h.

In seven subjects, it was not possible to shift the notch frequency by at least $\frac{1}{4}$ octave, because the frequency remained nearly the same even when the probe was withdrawn to the shallowest possible insertion. Since the primary objective of the experiment was to investigate the effect of changing the pressure distribution in the ear canal, the data from these seven subjects were excluded from further analysis. In seven other subjects, the SPL at threshold at one or more frequencies changed by more than 40 dB, probably because the subject fell asleep during the test. Because this threshold shift was larger than could be accounted for by the change in probe insertion depth, the data from these seven subjects were also excluded from further analysis. The data reported are from the remaining 61 subjects.

II. RESULTS

A. Probe

When chirp-response measurements were made in each of the five calibration tubes, the first resonant peaks occurred at 3.8, 4.6, 5.5, 6.3, and 7.1 kHz. The corresponding tube lengths, determined by the iterative procedure described

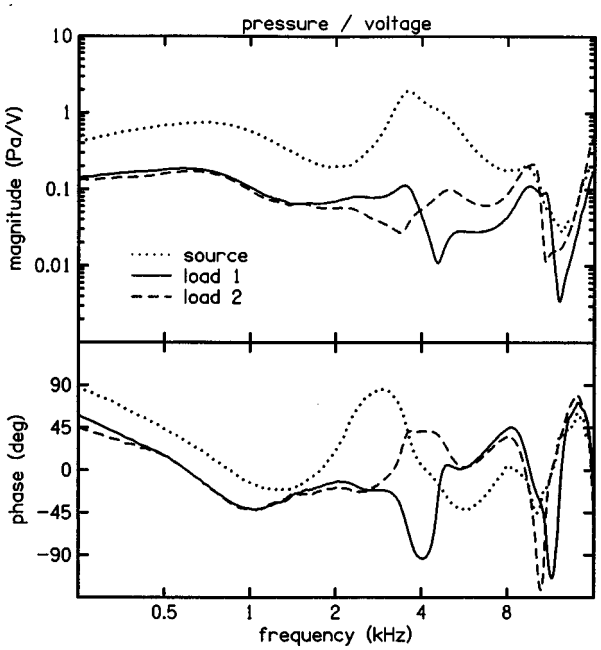

FIG. 1. Thevenin source and load pressures. The dotted lines represent the source pressure of the ER-10C. The solid and dashed lines represent the load pressure of the ear canal for the first and second insertions, respectively. The pressure magnitudes (upper panel) are normalized by the voltage to the probe. A linear phase, corresponding to a constant delay of 1.45 ms, was subtracted from all phase curves (lower panel) for clarity.

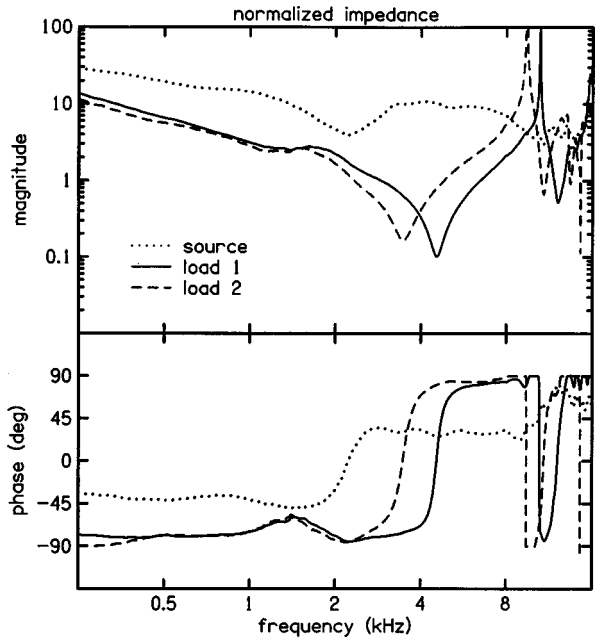

FIG. 2. Thevenin source and load impedance. The dotted lines represent the source impedance of the ER-10C probe. The solid and dashed lines represent the load impedance of the ear canal for the first and second insertions, respectively. The impedance magnitude (upper panel) is normalized by the characteristic impedance of the calibration cavities $Z_0 = 8 \times 10^6$ Pa/m^2 (=80 cgs acoustic ohms). The phase of the load impedance (lower panel) was restricted to the range between −90 and +90 by forcing the real part of the impedance to remain positive (see text).

above, were (on average) 45.2, 37.6, 31.1, 27.4, and 24.2 mm. The standard deviations associated with these tube lengths were 0.74, 0.78, 078, 0.78, and 0.77 mm, respectively. The similarity of these standard deviations across all of the different tube lengths suggests a common source of variability, such as the insertion depth of the probe tip into the coupler that was used for these calibrations.

The Thevenin acoustic source characteristics of ER-10C probe were obtained as a result of the calibration procedure. These computations were done in the frequency domain, with independent estimates for the source pressure and source impedance at each frequency. Typical results derived from one set of tube measurements are shown by the dotted lines in Figs. 1 and 2.

The source pressure/voltage ratio in Fig. 1 was computed by dividing the derived source pressure by the Fourier transform of the voltage waveform delivered to the probe. The magnitude of the source pressure (upper panel) decreases gradually between 0.5 and 8 kHz, except for a shallow dip around 2 kHz and a peak near 3.5 kHz. The phase (lower panel) has a corresponding peak near 3 kHz. A linear phase corresponding to a constant delay of 1.45 ms was subtracted from the measured phase to show details more clearly. Digital processing as the signal passes through the soundcard accounts for 1.21 ms of this delay. Electrical and acoustic propagation through the ER-10C accounts for the remaining (~0.24 ms) delay.

The source impedance in Fig. 2 was derived from the same tube measurements used to derive the source pressure shown in Fig. 1. The impedance magnitude is normalized by the characteristic impedance of the calibration tubes Z_0. The magnitude of the source impedance, like the pressure, is relatively constant across the frequency range of interest, except for a dip near 2 kHz. The phase has a 90-degree phase increase near 2 kHz, going from −45 degrees at low frequencies to +45 degrees at high frequencies. The magnitude and phase behavior near 2 kHz suggests that the ER-10C probe has an internal cavity that resonates at this frequency. The magnitude and phase functions should have a minimum-phase relationship because they represent the impedance of a physical system. Our tests to confirm this minimum-phase relation were inconclusive due to uncertainties about the impedance below 100 Hz and above 10 kHz.

Repeated measurements of the source pressure and impedance produced slightly different results. For example, across the 61 separate measurements on the same ER-10C probe, the normalized magnitude of the source impedance ranged from about 12 to 30 at 0.5 kHz and from about 2 to 9 at 8 kHz. These variations might be due to slight differences in compression of the foam eartip of the probe or due to instabilities in the analysis methods used to derive these quantities.

To access the accuracy of the probe calibration, the impedance of a test load of known impedance was also measured. The test load was a 60.0-mm brass tube of the same diameter (8.0 mm), but longer than any of the five tubes used for the probe calibration. Figure 3 compares the measured impedance of the test load (solid line) with the theoretical value calculated for this tube (Keefe, 1984). The agreement between the measured and the calculated impedances appears to be excellent from 0.5 to 8 kHz, which is the frequency range of interest.

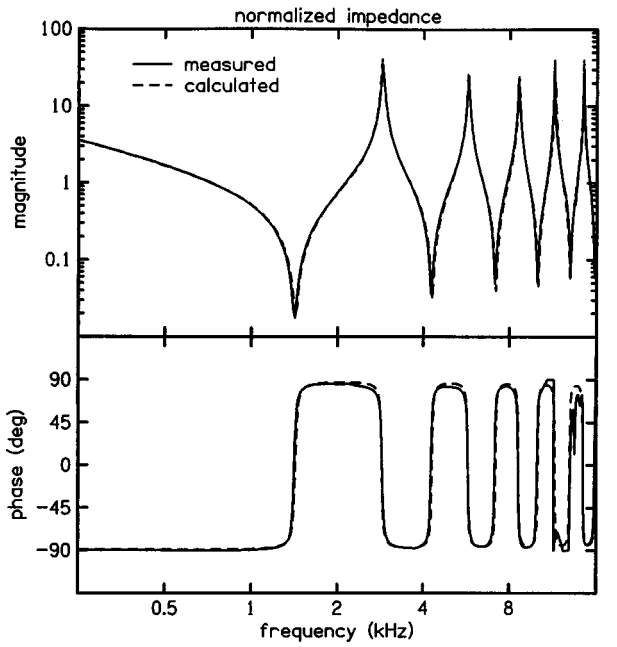

FIG. 3. Measured and calculated impedance for test load. The test load was a closed, brass tube at room temperature (25 °C) with 8-mm diameter and 60-mm length. The calculated impedance is based on equations from Keefe (1984). The impedance magnitude (upper panel) is normalized by $Z_0 = 8 \times 10^6$ Pa/m^2 (=80 cgs acoustic ohms).

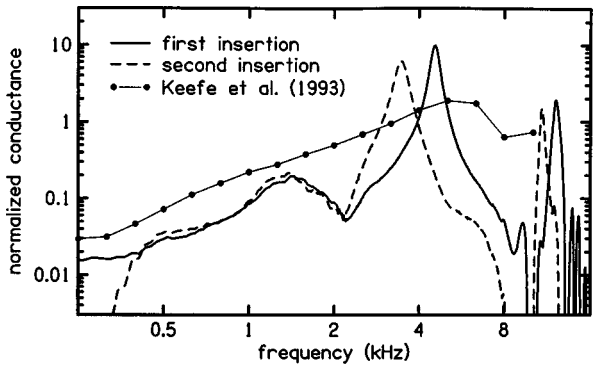

FIG. 4. Thevenin load conductance. The solid and dashed lines represent the conductance of the ear canal for the first and second insertions, respectively. These conductances correspond with the load impedance measurements shown in Fig. 2. The solid circles represent average, third-octave conductance values from ten adult subjects measured by Keefe *et al.* (1993). The conductance magnitude is normalized by Z_0, the characteristic impedance of the calibration cavities.

B. Ear canal

When the probe is inserted into an ear canal, the ear canal becomes the acoustic load being driven by the acoustic source within the probe. A typical measurement of an ear canal pressure is shown in Fig. 1. The solid line represents the first (deeper) insertion and the dashed line represents the second (shallower) insertion. The pressure/voltage ratio was computed by dividing the Fourier transform of the pressure waveform recorded from the probe by the Fourier transform of the voltage waveform delivered to the probe. Compared with the source pressure, the magnitude of the load pressure is generally smaller (by about 10 dB) and the phase shows no obvious difference in slope (that would be evidence of an additional delay).

The initial notch frequency can be seen in the pressure magnitude (solid line) at about 4.6 kHz. The notch moves down to about 3.3 kHz for the second insertion (dashed line). This shift of -0.4 octaves is a result of increasing the length of the air space between the plane of the probe and the eardrum. A downward shift of the notch frequency was observed in most subjects; however, in five subjects, the notch frequency shifted upward by more than 0.25 octaves. This was an unexpected result for which a definitive explanation is not known. We assume that the upward shift, occurring in 8% of our subjects, must be due to unusual curvature or cross-sectional area in these subjects' ear canals. While the upward shift is difficult to explain, its occurrence has no influence on the primary purpose of this shift namely, to determine the reliability of ear canal estimates of pressure and intensity. In the subset of 56 subjects where the notch frequency shifted downward (as expected), the initial notch frequency ranged from 3.4 to 8.1 kHz and the second notch frequency ranged from 2.6 to 5.3 kHz. In the other five subjects, where the notch frequency shifted upward, the initial notch frequency ranged from 2.4 to 6.2 kHz and the second notch frequency ranged from 3.2 to 8.4 kHz.

The solid and dashed lines in Fig. 2 show the ear canal normalized impedance corresponding to the ear canal pressure shown in Fig. 1. The ear canal impedance Z_{ec} at each frequency was computed from the probe pressure P_{prb}, probe impedance Z_{prb}, and ear canal pressure P_{ec}, according the formula $Z_{ec} = Z_{prb} \cdot P_{ec}/(P_{prb} - P_{ec})$. Note that the notch frequencies appear more distinct when they are observed in the impedance magnitude (Fig. 2) than when they are observed in the pressure magnitude (Fig. 1). This was always the case and made it easier (and more reliable) to determine the notch frequency from the impedance instead of the pressure. The impedance phase crosses zero at the notch frequency, going from -90 degrees at lower frequencies to $+90$ degrees at higher frequencies.

Occasionally, the phase of the impedance would become greater than $+90$ degrees or less than -90 degrees. For example, where the dashed line in the lower panel of Fig. 2 is equal to $+90$ degrees between 8 and 9 kHz, the computed impedance value was actually greater than $+90$ degrees. This meant that the real part of the complex impedance was negative, which was a nonphysical result for a passive system. The negative real impedance may have been due to measurement errors (noise), instability in the analysis methods used to compute the probe impedance, or changes in the probe impedance between probe calibration and ear canal insertion. The small amount by which the phase exceeded $+90$ degrees would have seemed insignificant when plotted, but the corresponding effect on the real part of the impedance greatly influences our estimate of acoustic intensity. Our method for dealing with these nonphysical impedances is described below.

The conductance values in Fig. 4 are for the same two probe insertions for which the pressure and impedance were presented in Figs. 1 and 2. Conductance is defined as the real part of $1/Z_{ec}$. Note that the conductance peaks in Fig. 4 occur at the notch frequencies of the pressure in Fig. 1 and the

impedance in Fig. 2. This means that if we know the frequency of the conductance peak, we also know the notch frequency. This method was used to determine the notch frequency for this experiment because it proved more reliable than using the pressure magnitude. For comparison, conductance values measured by Keefe *et al.* (1993) are also shown in Fig. 4.

When the real part of the impedance is negative, the conductance also becomes negative. In the example shown in Fig. 4, the conductance values were negative above 9.6 kHz for the first insertion (solid line) and above 8.1 kHz (and below 0.3 kHz) for the second insertion (dashed line). In this subject, the conductance values were positive over the frequency range of interest (0.5–8 kHz). However, in other subjects, negative conductance values sometimes occurred in the 0.5–8 kHz range. Dealing with negative conductance values presented the greatest challenge for this method of determining acoustic intensity in the ear canal. Because negative conductance values were considered unrealistic, a minimum (normalized) conductance value of 0.01 was established for the purpose of computing intensities. Whenever the conductance value was less than the minimum value, it was set equal to the minimum value. This adjustment made it possible to compute intensity values for all subjects at all frequencies of interest. Without this adjustment, 19 of the 61 subjects would have had negative values at one or more of the frequency at which behavioral thresholds were measured. This is not an ideal solution to the problem of negative conductance values. We hope that a better solution can be found to deal with this problem in the future.

The two ear canal pressure-to-voltage ratios shown in the upper panel of Fig. 1 as solid and dashed lines represent in-the-ear SPL calibrations. Using these curves, it is possible to determine the voltage needed to produce any desired SPL at any frequency. The differences in pressure-to-voltage ratio between the two insertion depths, by as much as an order of magnitude (20 dB) at some frequencies (near 4.2 kHz), illustrate the primary issue addressed in this paper. Specifically, in-the-ear SPL calibration cannot provide a reliable indication of the signal level entering the ear at some frequencies because it is so sensitive to the insertion depth of the probe.

Ear canal conductance provides the additional information needed to transform an SPL calibration into an SIL calibration. Figure 5 shows two in-the-ear SIL calibrations constructed from the pressure-magnitudes in Fig. 1 and the conductance in Fig. 4. The solid and dashed lines represent the first and second probe insertions, respectively. The difference between the two SIL calibrations in Fig. 5 is much smaller than the difference between the two SPL calibrations in Fig. 1. Multiplication by the conductance has effectively removed the ''standing-wave'' notches seen in SPL curves. The relative insensitivity of the SIL calibration to changes in probe insertion depth is an important advantage of this approach to calibration.

C. Thresholds

In Fig. 6, thresholds are shown for the five octave frequencies (0.5, 1, 2, 4, and 8 kHz). The circles indicate the mean values for the 61 subjects. The error bars indicate the

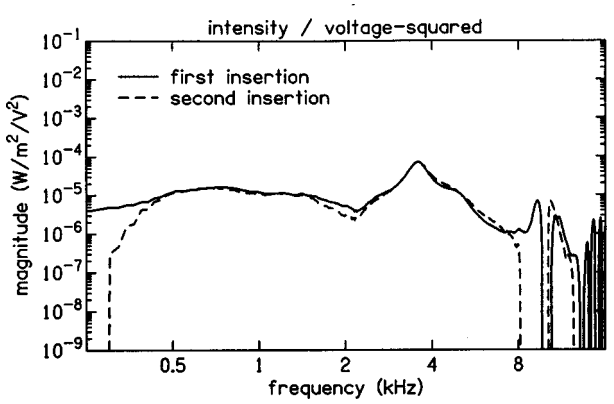

FIG. 5. Acoustic intensity in the ear canal. The solid and dashed lines represent the ratio of intensity in the ear canal to voltage squared at the probe for the first and second insertions, respectively. Note that intensity in the ear canal is less sensitive (between 0.5 and 8 kHz) to the change in probe insertion depth than the pressure magnitude shown in Fig. 1. To facilitate comparison, the vertical scales in Fig. 1 and in this figure both span an 80-dB signal range.

standard error of the mean. For each subject, the threshold values for the two probe insertions were averaged. The open circles indicate the sound pressure level (dB SPL) at threshold. For comparison, the triangles indicate the ANSI (1996) standard reference equivalent threshold (RETSPL) for an occluded ear simulator and the asterisks indicate the minimum audible pressure (MAP) at hearing threshold at the eardrum estimated by Killion (1978).

There is general agreement between the present mean thresholds and the average thresholds described in the na-

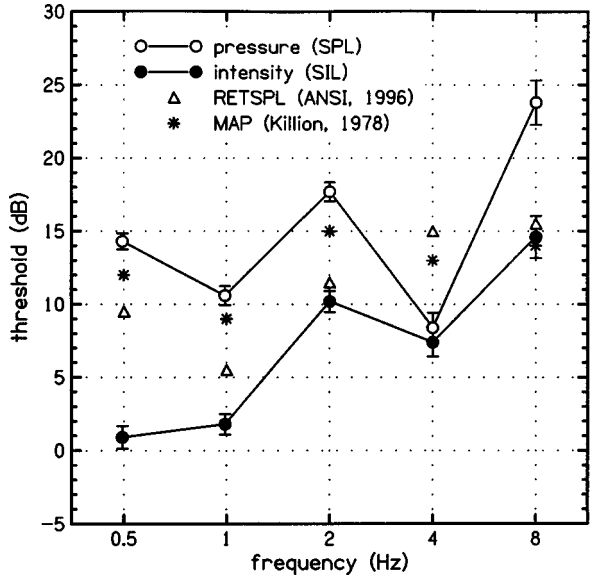

FIG. 6. Behavioral thresholds to tones. The open circles represent the mean SPL thresholds for our subjects in dB *re*: 20 μPa rms. The filled circles represent the mean SIL threshold in dB *re*: 10^{-12} W/m^2. (The filled circles also represent the mean power threshold in dB *re*: 5×10^{-17} W.) The SPL and SIL values were determined from the same threshold measurements using the ear canal conductance to convert SPL values to SIL values. The error bars indicate the standard error of the mean. For comparison, the triangles represent the ANSI (1996) reference equivalent thresholds (RETSPL) for an occluded ear simulator and the asterisks represent the minimum audible pressure (MAP) at the eardrum estimated by Killion (1978).

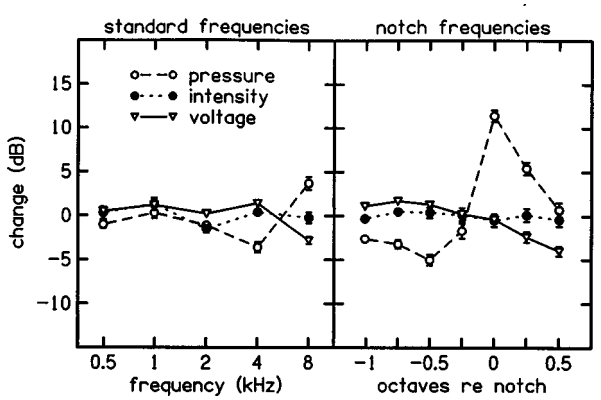

FIG. 7. SPL, SIL, and voltage threshold changes due to change of insertion depth. The open circles represent the mean change in SPL threshold, the closed circles represent the mean change in SIL threshold, and the triangles represent the change in voltage (dBV) to the probe at threshold. The error bars represent standard error of the mean. The five standard frequencies are shown in the left panel. The seven additional frequencies near the notch frequency are shown in the right panel.

tional standards and by Killion. The present threshold values were higher than the previously published values, except at 4 kHz. This is probably descriptive of the subjects population, since normal hearing was not a requirement for inclusion in this study. The lower threshold in our subjects at 4 kHz is probably an artifact of the spectral notch in pressure magnitude that was usually observed at frequencies near 4 kHz.

The filled circles show the sound intensity level (SIL) at threshold expressed in dB *re:* 1 pW/m^2. No standard for the SIL at behavioral threshold has yet been established for use with insert earphones. The threshold SIL is not constant across frequency; it is 13.7 dB higher at 8 kHz than at 0.5 kHz, suggesting a trend for the threshold SIL to increase with frequency by about 3 dB/octave. This is greater than the change in MAP, which is only 2 dB larger at 8 kHz than at 0.5 kHz.

The change in threshold between the two probe insertions is shown in Fig. 7. The open circles indicate the mean SPL change and the filled circles indicate the mean SIL change. The error bars represent the standard error of the mean. Results of the five octave frequencies (0.5, 1, 2, 4, and 8 kHz) are shown in the left panel, while the threshold changes at the seven additional frequencies (-1, $-\frac{3}{4}$, $-\frac{1}{2}$, $-\frac{1}{4}$, 0, $\frac{1}{4}$, and $\frac{1}{2}$ octaves relative to the initial notch frequency) are shown in the right panel. At 2 kHz and below (left panel), the mean threshold change at the standard frequencies is about 1 dB or less for both SPL and SIL measures of threshold. The difference between SPL and SIL is less than 1 dB at 2 kHz and below. The mean SPL change decreases by about 3 dB at 4 kHz and increases by about 3 dB at 8 kHz. These deviations are probably due to the reflection of sound waves at the eardrum. The mean SIL change is less than 1 dB at 4 and 8 kHz.

A greater contrast between the mean SPL change and the mean SIL change is seen in the right panel of Fig. 7. The fact that the SPL change is negative for frequencies below the initial notch frequency is evidence of the downward shift of the notch frequency by about $\frac{1}{2}$ octave for the second probe insertion. The mean SPL change is most positive (11.4 dB) at the initial notch frequency and most negative (-5.0 dB) at one-half octave below this frequency. By contrast, the SIL change is never more than ± 0.5 dB at any frequency in the vicinity of the notch frequency. Since we assumed that behavioral thresholds have not changed between the two probe insertions, the large SPL changes must indicate that the SPL at the plane of the probe differs from the SPL at the eardrum.

An alternative to in-the-ear calibration (SPL or SIL) is to calibrate the insert earphone in an occluded ear simulator or other coupler attached to a calibrated microphone (ANSI, 1996). With this calibration method, the voltage required to produce a given SPL in the coupler is assumed to produce the same SPL at the eardrum. To assess the effect of using a voltage reference in place of in-the-ear calibration, the triangles in Fig. 7 show the mean change in voltage (dBV) delivered to the earphone at threshold. In general, the voltage change appears to be less than the SPL change, but greater than the SIL change. This suggests that a voltage reference may be more reliable than in-the-ear pressure calibration, especially for frequencies at which a notch in the SPL occurs; however, calibrating the voltage reference presents its own set of problems, as discussed below.

III. DISCUSSION

The method used to obtain ear canal impedance by first determining the Thevenin acoustic source characteristics generally follows the description provided by Allen (1986) and Keefe *et al.* (1992). The choice of five calibration tubes was a compromise between the four tubes recommended by Allen and the six tubes recommended by Keefe. The tube lengths also represent a compromise between the slightly shorter tubes used by Voss and Allen (1994), which ranged from 11.2 to 30.2 mm, and the much longer tubes used by Keefe *et al.* (1992), which ranged from 238 to 500 mm. The tube lengths used in this study were selected so that the frequencies of the first resonant peaks (at the half-wave resonance) would span the frequency range of greatest interest (4–8 kHz) with approximately uniform spacing.

Our decision to heat the calibration tubes to body temperature was based on a suggestion by Allen (personal communication) and some preliminary comparisons that we made between calibrations performed at room temperature and at body temperature. We observed phase shifts in the source impedance and source pressure as the temperature was raised from room temperature to body temperature. These phase shifts were larger at higher frequencies and were consistent with the increased speed of sound due to the temperature increase. More importantly, negative conductance values occurred less frequently in our initial tests when the probe calibration was performed at the same temperature as the test load. While this result was not definitive, it did suggest that heating our calibration tubes to body temperature for this study might be worth the effort.

Others have demonstrated that probe calibration is possible using only two acoustic loads (e.g., Rosowski *et al.*, 1990; Puria *et al.*, 1997; Lynch *et al.*, 1994). The two-load method was not used in this study because it was not known whether the unevenness and inconsistency of the foam tip on

the ER-10C would interfere with the accurate determination of effective tube lengths. There was also some concern about the effect of temperature on the calibration. When the tube lengths are determined by an iterative procedure, a small error in the temperature specification can be partially corrected by adjusting the effective tube length appropriately. The only successful probe calibrations for the ER-10C that were known at the time that this study was initiated were those of Allen (personal communication) using four tubes and Keefe (personal communication) using six tubes, which formed the basis for the selection of five tubes for this study.

An independent calibration of the ER-10C probe was recently reported by Huang *et al.* (1998). Huang *et al.* recommend that the ER-10C probe be modified to extend the microphone tube 3–4 mm beyond the earphone tube to reduce evanescent effects, which were found to be significant (see also Rabinowitz, 1981). This may represent a source of calibration error in the present study, since we did not modify the microphone tube in this manner. For example, the small phase errors we observed between measured and calculated impedance values (see Fig. 5) might be due to evanescent effects.

The probe calibration procedure used in this study appears to be efficient and reliable in most cases. However, the large number of subjects for which negative conductance values occurred at frequencies of interest (19 out of 61) suggests that some improvement in this method is warranted before it is adopted for routine use. Incorporation of additional physical constraints (perhaps by physical modeling) may be useful. The results of the experiment would have been nearly the same if we had excluded the 19 subjects with negative conductance, suggesting that the main effects we observed were robust. Including all 61 subjects in the data analysis (by setting a minimum value for the conductance) gives a more realistic assessment of the results that can be obtained by currently available methods.

The Thevenin acoustic source pressure and impedance shown in Figs. 1 and 2 have not previously been published for the ER-10C; although source reflectance, derived from the source impedance, has been published by Keefe (1997). Informal comparisons were made of the Thevenin source impedance shown in Fig. 2 with that obtained (using similar methods) by Allen (personal communication) and Keefe (personal communication) for the ER-10C. Results of these comparisons indicate as much as a factor of 3 difference between the lowest and highest impedance values at any given frequency. This discrepancy is about the same as the range of values across the 61 probe calibrations obtained in this experiment alone. The variability in results among these probe calibrations can be attributed to variations in the eartip, instabilities in the analysis methods, and, in the comparisons with Allen's and Keefe's results, physical differences among the different ER-10C probes. Significantly better agreement among source impedance estimates should be possible with improvements in the methods used to derive the Thevenin source characteristics.

In Fig. 6, the difference between the ANSI standard RETSPL and the mean value of our measured SPL at threshold is about 4 dB at 500 Hz and increases to about 8 dB at 8 kHz. There may be several reasons for this discrepancy: (1) The occluded ear simulator used in the ANSI standard might not be representative of the average ear canal of our subjects. Note that below 8 kHz, our group means are closer to Killion's MAP than the RETSPL. Killion's MAP values have been confirmed in a comparison with other studies (Wilbur *et al.*, 1988) and may be more reliable than the ANSI RETSPL values. (2) Our technique measures SPL at the probe whereas ANSI standard and Killion's MAP both refer to SPL at the eardrum. (3) The average threshold of our subjects was probably not exactly 0 dB HL (*re*: ANSI, 1996) at all frequencies. We did not obtain (standard clinical) audiometric thresholds on these subjects because the focus of this experiment was on threshold changes rather than absolute thresholds. Finally, (4) there may be errors or biases in our threshold measurement methods. One possible source of measurement error is subject inattention. Failure to respond to audible tones inappropriately elevates the threshold estimate obtained by our automated threshold procedure. Another possible source of measurement error is the deviation of the ER-10C microphone calibration from a constant value. In our calculations, we assumed that the microphone sensitivity was 0.05 V/Pa at all frequencies. The calibration chart for this microphone supplied by the manufacturer indicates that the error in this assumption is at most 1 or 2 dB over the frequency range of interest (0.5–8 kHz).

In Fig. 4, we compare our measured conductance values for one subject with the third octave conductance values obtained by Keefe *et al.* (1993) for the mean of ten subjects. Below 2 kHz, the conductance values obtained by Keefe *et al.* are similar to those obtained by Møller (1960), who also presented the mean of ten subjects, but did not measure above 2 kHz. The mean conductance values of Keefe *et al.* do not show the distinct peaks and dips that are apparent in the conductance of a single ear canal; however, an average of the conductance values we obtained in all 61 subjects would be similar to their mean value.

In-the-ear pressure calibration is the method currently used by most commercial DPOAE measurement systems. Siegel (1994) has shown that such calibration can lead to significant errors in the measured DPOAE amplitudes. The reason for the DPOAE amplitude errors is that the stimulus levels measured at the plane of the probe were not always a good indication of the stimulus level at the eardrum. The results shown in Figs. 5 and 7 indicate that in-the-ear intensity calibration would not have the same problems as pressure calibrations and could, therefore, lead to more reliable measures of DPOAE amplitude because the stimulus level would be more reliably determined. This improvement in accuracy of the stimulus level is obtained despite the problems with current methods (such as negative conductance) described above.

One disadvantage of using in-the-ear intensity calibration is the additional time (5–10 min) required to recalibrate the probe before each ear canal measurements. It is, therefore, of interest of know whether similar results could be obtained with fewer probe calibrations. We repeated the analysis using the same probe calibration (the one illustrated

in Figs. 1, 2, and 4) for all ears. The mean SPL and SIL values for the change in threshold were within 1 dB of the values shown in Fig. 7, despite a much more frequent occurrence of negative conductance values. Thus, it appears that in-the-ear SIL calibration retains its advantage over SPL calibration even with a single probe calibration.

An alternative to in-the-ear calibration is to calibrate the probe in an occluded ear simulator or other coupler attached to a calibrated microphone. With this method, the voltage that produces the desired SPL in the coupler would be assumed to produce the same SPL in the ear canal. To assess this calibration method, it is of interest to know whether a given voltage to the earphone always produces the same level of sound entering the ear. The triangles in Fig. 7 show that the change in threshold is greater at most frequencies for a voltage reference than it is for an intensity reference. The voltage change is greatest at 8 kHz or above the notch frequency. In general, based on these results, it would appear that coupler calibration may be preferable to in-the-ear SPL calibration, but not as good as in-the-ear SIL calibration. However, there are other problems associated with coupler calibrations. For example, if the coupler impedance is much different than the ear-canal impedance, then the pressure measured in the coupler (by the calibration microphone) can be much different than the pressure presented to the eardrum. Thus one could obtain errors from coupler calibrations that are as large as those observed with in-the-ear pressure calibrations.

If intensity is a better indicator of stimulus level than pressure, then the question arises whether the ear is detecting pressure or power. In Fig. 6, we see that neither the pressure nor the intensity at threshold is constant across frequency. Puria *et al.* (1997) provided evidence from measurements in human cadaver ears that behavioral threshold corresponds to constant pressure (28 dB SPL) in the vestibule of the cochlea. With this observation in mind, we can interpret our results in the following way. Pressure at the probe is not constant at threshold across frequency because it is not a good indicator of pressure in the cochlea, due to reflected waves from the eardrum and middle ear. Intensity at the probe is not constant across frequency because the ear is not a power detector.

If behavioral threshold is determined by pressure at the entrance to the cochlea (Puria *et al.*, 1997), then calibrating sound levels to a pressure reference may be preferable to using an intensity reference. Direct measurement of pressure at the eardrum avoids the problem of notches due to standing waves (Siegel, 1994), but the procedure may be too difficult for routine use. Another way to obtain estimates of pressure at the eardrum is to use a calibrated probe, estimate the ear canal diameter and distance between the probe and the eardrum, and calculate the propagated pressure at the eardrum assuming cylindrical geometry (Rabinowitz, 1981; Huang *et al.*, 1988; Stevens *et al.*, 1987).

IV. CONCLUSIONS

Currently available methods for estimating acoustic source pressure and impedance of a probe allow the determination of sound intensity level (SIL) in addition to sound pressure level (SPL) in the ear canal. Above 2 kHz the in-the-ear SIL measurement appears to provide a better indication of the level of sound entering the ear than in-the-ear SPL calibration, judged by the sensitivity of behavioral thresholds to changes in probe insertion depth. Coupler calibration may be better than in-the-ear SPL calibration, but does not appear to be as good as in-the-ear SIL calibration. Below 2 kHz, SIL and SPL calibrations appear to perform equally well.

ACKNOWLEDGMENTS

Jan Kaminski performed the measurements on all subjects included in this study. Douglas Keefe, Huanping Dai, Meade Killion, and an anonymous reviewer made many helpful suggestions for improvements in this paper. This work was supported by a grant (P60-DC00982) from the National Institutes of Health.

Allen, J. B. (**1986**). ''Measurement of eardrum acoustic impedance,'' in *Peripheral Auditory Mechanisms*, edited by J. B. Allen, J. L. Hall, A. Hubbard, S. T. Neely, and A. Tubis (Springer-Verlag, New York).

ANSI (**1996**). ANSI S3.6-1996, ''Specifications for audiometers'' (American National Standards Institute, New York).

Green, D. M. (**1993**). ''A maximum-likelihood method for estimating thresholds in a yesno task,'' J. Acoust. Soc. Am. **93**, 2096–2105.

Green, D. M. (**1995**). ''Maximum-likelihood procedures and the inattentive observed,'' J. Acoust. Soc. Am. **97**, 3749–3760.

Huang, G. T., Rosowski, J. J., Puria, S., and Peake, W. T. (**1998**). ''Noninvasive technique for estimating acoustic impedance at the tympanic membrane (TM) in ear canals of different size,'' Assoc. Res. Otolaryngol. Abs. **21**, 487.

Keefe, D. H. (**1984**). ''Acoustical wave propagation in cylindrical ducts: Transmission line parameter approximations for isothermal and nonisothermal boundary conditions,'' J. Acoust. Soc. Am. **75**, 1386–1391.

Keefe, D. H., Ling, R., and Bulen, R. C. (**1992**). ''Method to measure acoustic impedance and reflection coefficient,'' J. Acoust. Soc. Am. **75**, 1386–1391.

Keefe, D. H. (**1997**). ''Otoreflectance of the cochlea and middle ear,'' J. Acoust. Soc. Am. **102**, 2849–2859.

Keefe, D. H., Bulen, J. C., Hoberg, K., and Burns, E. M. (**1993**). ''Ear-canal impedance and reflection coefficient of human infants and adults,'' J. Acoust. Soc. Am. **94**, 2617–2638.

Killion, M. C. (**1978**). ''Revised estimate of minimum audible pressure: Where is the missing 6 dB?'' J. Acoust. Soc. Am. **63**, 1501–1508.

Lynch, T. J. III, Peake, W. T., and Rosowski, J. J. (**1994**). ''Measurement of the acoustic input impedance of cat ears: 10 Hz to 20 kHz,'' J. Acoust. Soc. Am. **96**, 2184–2209.

Marlan, R. S., Kim, D. O., LaBrie, L., and Leonard, G. (**1994**). ''Specification of high frequency stimulus level in terms of acoustic power using Thevenin equivalent source in the measurement of DPOAEs,'' Assoc. Res. Otolaryngol. Abs. **17**, 55.

Møller, A. R. (**1960**). ''Improved technique for detailed measurements of middle-ear impedance,'' J. Acoust. Soc. Am. **32**, 250–257.

Pierce, A. D. (**1981**). *Acoustics: An Introduction to its Physical Principles and Applications* (McGraw-Hill, New York), p. 107.

Puria, S., Peake, W. T., and Rosowski, J. J. (**1997**). ''Sound-pressure measurements in the cochlear vestibule of human-cadaver ears,'' J. Acoust. Soc. Am. **101**, 2754–2770.

Rabinowitz, W. M. (**1981**). ''Measurement of the acoustic immittance of the middle ear,'' J. Acoust. Soc. Am. **70**, 1025–1035.

Rosowski, J. J., Davis, P. J., Merchant, S. N., Donahue, K. M., and Coltrera, M. D. (**1990**). ''Cadaver middle ears as models for living ears: comparisons of middle ear input, immittance,'' Ann. Otol. Rhinol. Laryngol. **99**, 403–412.

Siegel, J. H. (**1994**). ''Ear-canal standing-waves and high-frequency sound calibration using otoacoustic emission probes,'' J. Acoust. Soc. Am. **93**, 3308–3319.

Siegel, J. H., and Hirohata, X. (**1994**). ''Sound calibration and distortion product otoacoustic emissions at high frequencies,'' Hearing Res. **80**, 146–152.

Stevens, K. N., Berkovitz, R., Kidd, Jr., G., and Green, D. M. (**1987**). ''Calibration of ear canals for audiometry at high frequencies,'' J. Acoust. Soc. Am. **81**, 470–484.
Voss, S. E., and Allen, J. B. (**1994**). ''Measurement of acoustic impedance and reflectance in the human ear canal,'' J. Acoust. Soc. Am. **95**, 372–384.
Wilber, L. A., Kruger, B., and Killion, M. C. (**1988**). ''Reference thresholds for the ER-3A insert earphone,'' J. Acoust. Soc. Am. **82**, 669–676.